Solute Effects on the Colloidal and Phase Behavior of Lipid Bilayer Membranes: Ethanol-Dipalmitoylphosphatidylcholine Mixtures

Ulrich Vierl, Ludwig Löbbecke, Norbert Nagel, and Gregor Cevc
Medizinische Biophysik, Technische Universität München, Klinikum r.d.l., D-81675 München, Germany

ABSTRACT By means of the scanning differential calorimetry, x-ray diffractometry, and the dynamic light scattering, we have systematically studied the phase and packing properties of dipalmitoylphosphatidylcholine vesicles or multibilayers in the presence of ethanol. We have also determined the partial ternary phase diagram of such dipalmitoylphosphatidylcholine/water/ethanol mixtures. The directly measured variability of the structural bilayer parameters implies that ethanol binding to the phospholipid bilayers increases the lateral as well as the transverse repulsion between the lipid molecules. This enlarges the hydrocarbon tilt (by up to 23°) and molecular area (by ≤40%). Ethanol-phospholid association also broadens the interface and, thus, promotes lipid headgroup solvation. This results in excessive swelling (by 130%) of the phosphatidylcholine bilayers in aqueous ethanol solutions. Lateral bilayer expansion, moreover, provokes a successive interdigitation of the hydrocarbon chains in the systems with bulk ethanol concentrations of 0.4–1.2 M. The hydrocarbon packing density as well as the propensity for the formation of lamellar gel phases simultaneously increase. The pretransition temperature of phosphatidylcholine bilayers is more sensitive to the addition of alcohol (initial shift: ΔT_p = 22°C/mol) than the subtransition temperature (ΔT_s = 5°C/mol), whereas the chain-melting phase transition temperature is even less affected (ΔT_m = 1.8°C/mol). After an initial decrease of 3 degrees for the bulk ethanol concentrations below 1.2 M, the T_m value increases by 2.5 degrees above this limiting concentration. The gel-phase phosphatidylcholine membranes below T_m are fully interdigitated above this limiting concentration. The chain tilt on the fringe of full chain interdigitation is zero and increases with higher ethanol concentrations. Above T_m, some of the lipid molecules are solubilized by the bound ethanol molecules. More highly concentrated ethanol solutions (>7 M) solubilize the phosphatidylcholine bilayers with fluid chains fully and result in the formation of mixed lipid-alcohol micelles.

INTRODUCTION

Lipid phase behavior in water has been studied in detail (for a general overview see, for example, Cevc and Marsh, 1987). Many phase transitions (subtransition, pretransition, chain-melting phase transition, transition from a lamellar into a nonlamellar state) have been reported. Most of these are now well understood. One of the notable exceptions is the bilayer-to-interdigitated-bilayer phase transition (for a review, see Slater and Huang, 1988). Such a transition can be induced by a variety of molecules ranging from the bare anions or simple alcohols through to the more complex systems such as polyalcohols (McDaniel et al., 1983) or polypeptides (Ranck and Tocanne, 1982).

Because of their simple structure, alcohols are, perhaps the best candidate for the systematic studies of the solute-induced lipid-chain interdigitation. By varying the length of the aliphatic chain, the relative hydrophobicity of such transition inducers can be varied easily; by changing the number and/or the position of the alcohol residues, the site and the strength of molecular hydrophilicity can be modified.

The influence of alcohols on the pretransition temperature (T_p), on the chain-melting phase transition temperature (T_m), and on the induced chain interdigitation of several phospholipids (chiefly phosphatidylcholines; PCs) has been investigated (Rowe and Cutrera, 1987; Veiro et al., 1988; Nambi et al., 1988; Rowe, 1983, 1985, 1987; Simon and McIntosh, 1984; McIntosh et al., 1989; Ohki et al., 1990). The partitioning of the alcohol molecules between an organic and an aqueous subphase has also already been the topic of interest (Rowe, 1983). Recent FTIR measurements, for example, have shed some light on the probable location of the ethanol molecules in the interfacial region (Chiou et al., 1992).

In one of the first studies of the interaction between the ethanol and phosphatidylcholine molecules (Rowe, 1983), a "biphasic" effect on the lipid chain-melting phase transition temperature (T_m) has been reported. T_m was first seen to decrease and then to increase with increasing bulk ethanol concentration.

X-ray diffraction measurements (Simon and McIntosh, 1984) on similar systems have revealed that the "biphasic" effect is caused by the lipid chain interdigitation. The ethanol sensitivity of the lipid chain-melting phase transition temperatures was thus explained in terms of the higher partitioning of the ethanol molecules between the lipid and the aqueous phase in fluid bilayer membranes. In the later studies of ethanol-induced chain interdigitation (Rowe and Cutrera, 1987; Nambi et al., 1988; Veiro et al., 1987), a concomitant downward shift of the pretransition temperature was found. Nambi, Rowe and McIntosh were the first who proposed a rather complete phase diagram for the DPPC- and DSPC-ethanol system (Nambi et al., 1988). The disappearance of the lipid-pretransition upon hydrocarbon interdigitation has also been reported for the mixed-chain phosphatidylcholines (Mattai et al., 1987; Lin et al., 1991).

Received for publication 5 November 1993 and in final form 6 June 1994.
Address reprint requests to Gregor Cevc, Mediziniche Biophysik, Technische Universität München, Klinikum rechts der Isar Ismaningerstr 22, D-81675 München BR Germany. Tel.: 011-49-89-4140-2544; Fax: 011-49-89-4180-5179; E-mail: TB80201@SUNMAIL.LRZ-MUENCHEN.DE.

0006-3495/94/09/1067/13 $2.00

We have studied DPPC/ethanol mixtures by using differential scanning calorimetry (DSC), dynamic light scattering (DLC), and small angle x-ray diffractometry. The resulting wealth of data has permitted us to construct a detailed phase diagram of the DPPC/ethanol/water mixtures between 5 and 80°C. Our chief motivation for this was the desire to understand in detail the mechanism of the solute-induced lipid chain interdigitation. Our secondary goal was to highlight the ethanol/DPPC interactions at the molecular scale.

In brief, we have found that the phase diagram of ethanol-PC mixtures can be separated into four major domains depending on the bulk alcohol concentration. 1) At low alcohol concentrations, the tilt angle of the hydrocarbon chains is increased by the presence of ethanol molecules to a maximum value of ~50° ($L_{\beta'}$ phase in this region is thus really a family of $L_{\beta'}$ phases with different tilt angles; the area per lipid headgroup concomitantly increases and the lipid bilayer thickness simultaneously decreases in this phase. This does not affect the sequence of phases but significantly lowers the temperatures of all transitions that involve lipids in a gel-phase.) 2) A further increase of the bulk ethanol concentration gives rise to the coexistence of interdigitated and noninterdigitated hydrocarbon chains. The corresponding domains appear to be distributed throughout the lipid bilayer so that the $L_{\beta'}$-phase ($P_{\beta'}$-phase) is now replaced by a combination of the $L_{\beta'}$ + $L_{\beta i}$-phases ($P_{\beta'}$ + $L_{\beta i}$-phases). 3) At ethanol concentrations higher than ~1.2 M EtOH, all hydrocarbon chains of PCs are fully interdigitated. No normal bilayers are observed in this ethanol concentration range at temperatures between the lipid subtransition and the chain-melting phase transition temperature. 4) Very high ethanol concentrations solubilize lipids in the fluid-lamellar phase. (Metastable) lipid vesicles can coexist with the mixed ethanol/PC micelles, however.

MATERIALS AND METHODS

Materials

1,2-Dipalmitoyl-*sn*-glycero-3-phosphocholine (DPPC, purity >99%) was purchased from Boehringer (Mannheim, Germany). Ethanol (EtOH, p.a.) was obtained from Merck (Darmstadt, Germany). Water (18 MΩ/cm) was doubly distilled in an all-glass apparatus and reprocessed by a water purification unit (Elgastat HQ, UK).

Differential scanning calorimetry measurements

Multilamellar vesicles for the DSC measurements were prepared by adding DPPC to bidestilled water. The resulting suspension (usually 5 mM DPPC, with higher lipid concentrations being used for the determination of lipid subtransition temperatures) was heated to 50°C for at least 1 h and occasionally vortexed. Subsequent sample aging at room temperature for one week ensured a good sample homogeneity. Appropriate ethanol amounts were then added to the aged lipid suspensions 2 h before each measurement. Longer equilibration periods had no measurable effect on the experimental results.

DSC measurements were done in a MC2 scanning calorimeter (MicroCal, Inc., Amherst, MA) with the original data acquisition and analysis software (ORIGIN). For the cooling-scan measurements, the calorimeter was connected to a computer-controlled refrigerated bath (F3C, Haake, Germany). Samples were heated and cooled in the temperature range 4–50°C at scanning rates of 30 K/h and 20 K/h, respectively. To determine the subtransition temperature, samples were stored at 4°C before each measurement for at least 10 days.

X-ray diffraction

10 mg of DPPC were dissolved in 80 μl of the water-ethanol mixture of known composition. After swelling for several hours above the chain-melting transition temperature, the resulting suspension of multilamellar vesicles was hermetically sealed in an x-ray glass capillary with a wall thickness of 0.01 mm (W. Müller, Berlin, Germany). Best results were obtained with capillaries of 1.5-mm diameter.

In a Guinier x-ray diffraction camera (Huber Diffraktionstechnik, Rimsting, Germany), the radiation from a Cu-standing anode was focused by a quartz monochromator onto the sample-containing capillary, placed in a brass holder. Temperature of the latter was controlled with an accuracy of 0.1°C with a temperature controller (Eurotherm, Limburg/Lahn, Germany). Scattered radiation was focused on a cylindrical film holder positioned after a horizontal slit or on the position-sensitive counter (Braun, Garching b.M., Germany). By lifting the film-holder and simultaneously changing the sample temperature, continuous temperature scans were recorded. Evaluation of x-ray photographs was done with a vernier calliper or on a scanning-microdensitometer (Biomed Instruments). Data from the position-sensitive detector were corrected to allow for the background radiation and geometric factors from the camera and the detector. Integrated intensities were calculated by standard procedures (Blaurock and Worthington, 1966).

Dynamic light scattering experiments

To prepare the samples for the optical measurements, suspensions of multilamellar lipid vesicles in doubly distilled water (50 mg of DPPC/ml) were sonicated (Heat Systems W 380) at 42°C until the average vesicle diameter was approximately 50–60 nm. The resulting suspension of largely unilamellar liposomes was pressed through a sterile 0.2-μm filter (Sartorius, Göttingen, Germany) and stored at room temperature.

Alternatively, small unilamellar vesicles were prepared by multiple manual extrusion through a 0.1 μm pore filter (Nucleopore) by using a LiposoFast device (Avestin, Ottawa, Canada). Vesicle size in the resulting (sterile) preparation was controlled before each experiment; it remained stable for several weeks, at least. According to our scanning calorimetric data, all investigated vesicles were in the $L_{\beta'}$ phase at 25°C, in the $P_{\beta'}$-phase at 37°C, and in the L_{α}-phase at 50°C.

Samples for the dynamic light scattering experiments were prepared by diluting 20 μl of the original lipid suspension in 1 ml of the appropriate ethanol/water mixture. This yielded final lipid concentrations between 0.5 and 1 mM. Just before a measurement, each sample was filtered through a 0.2 μm Millex GV13 filter (Millipore) into an acryl, 1 cm light-path cuvette. (The latter was prewashed twice with a freshly filtered water.) Finally, the cuvette was sealed with two layers of parafilm. (Contamination-free preparation of all samples for the light-scattering experiments as well as manipulation in a dust-free environment were found to be essential for the high quality and the reproducibility of DLS measurements.)

For the size determinations above room temperature, all samples were exquilibrated for 12 h at 37°C ($P_{\beta'}$-phase) or at 50°C (L_{α}-phase).

Dynamic light scattering measurements were done in triplicate using a Zetasizer 2C instrument (Malvern Instruments, Malvern, UK) equipped with a thermostated (±1 degree) sample cell. Data were analyzed by the multi-tau procedure from the Autosizer software package. The required solvent viscosities were taken from Weast and Astle (1986). The increase of the refraction index of the ethanol-water mixtures in the examined concentration range (0–2 M EtOH) is only 4 per mil (Weast and Astle, 1986) and, therefore, can be ignored.

RESULTS

Differential scanning calorimetry

The influence of ethanol on the phase behavior of DPPC was first investigated by differential scanning calorimetry. By this method, the alcohol-induced shifts of the temperature and the enthalpy of the lipid subtransition (T_c, $L_{c'} \rightarrow L_{\beta'}$), the pretransition ($T_p$, $L_{\beta'} \rightarrow P_{\beta'}$) and the chain-melting phase transition (T_m, $P_{\beta'} \rightarrow L_\alpha$, $L_{\beta'} \rightarrow L_\alpha$) were studied in detail.

In Fig. 1, the values of sub-, pre-, and chain-melting phase transition temperatures are given. The subtransition temperature of DPPC in water is 18.2°C. According to our experiments, this value remains essentially constant even in 1.2 M aqueous ethanol solutions (Füldner, 1981). Higher ethanol concentrations depress the subtransition temperature linearly, however, T_s = 15°C being measured in 2 M ethanol. The half-width of subtransition (3.2°C) is unaffected by the bulk ethanol concentration. Between two heating circles, the equilibration time at 4°C was 1 h. This does not suffice for a complete crystallization of the DPPC chains in water, the previously reported recovery times for the subtransition in such system being in the range of days or even weeks (Ruocco and Shipley, 1982). It is interesting, therefore, to note that we have repeatedly observed a small peak at $T = T_s$ upon the second heating of the sample in the presence of more than 1.2 M ethanol. Systematic investigation of this effect has revealed that after an equilibration period of 10 or 36 h in 1.6 M ethanol, the observed peak enthalpy reaches 25 or 75%, respectively, of the value measured in the first scan. (By x-ray measurements, we have verified that these peaks, indeed, stem from the lipid subtransition.) The average enthalpy of the DPPC-subtransition is approximately 16.5 kJ/mol and is independent of the bulk ethanol concentration (after 14 days of storage at 4°C).

The pretransition temperature of DPPC in water is 34.5°C. In the presence of as little as 0.1 mol of ethanol per liter of water, this value decreases linearly to 29.5°C, however. Further increase of the bulk ethanol concentration results in a rather smooth, but small, decrease of the pretransition temperature to 28.8°C. This value is measured with DPPC in 0.54 M aqueous ethanol. More concentrated ethanol decreases the pretransition temperature more steeply, down to an absolute minimum of 26.6°C in 0.9 M EtOH. Even higher ethanol concentrations first very steeply increase the T_p-value to 27.5°C in 1.1 M EtOH, where the pretransition becomes undetectable.

The pretransition enthalpy of DPPC (see Fig. 2) in excess water is approximately 5 kJ/mol. According to our measurements, this value is not affected by the presence of ethanol at concentrations lower than 0.55 M. Ethanol concentrations higher than this, however, linearly decrease the enthalpy of the DPPC pretransition to zero.

Upon the addition of ethanol to suspensions of DPPC in water, the chain-melting phase transition temperature first decreases linearly with the bulk ethanol concentration from 41.2°C in water to 39.8°C in 1.1 M ethanol. Higher ethanol concentrations then shift this temperature back to 41.5°C (in 1.74 M ethanol). The chain-melting enthalpy first gets higher by the presence of ethanol: from a value of 40 kJ/mol in water, it rises to 48.8 kJ/mol in 0.9 M aqueous ethanol. A gradual increase of the bulk ethanol concentration to 2 M, however, decreases this enthalpy value linearly to 41 kJ/mol.

The shape of calorimetric peaks pertaining to the chain-melting phase transition of DPPC in the presence of ethanol is very similar in the heating and cooling scans. Appreciable hysteresis between the up- and downscan is typically observed, however, when the chain interdigitation is complete. In this respect, our data are similar to those published by other groups (Rowe, 1985).

The pretransition as well as the main transition of DPPC bilayers are both broadened by the presence of ethanol. The half-width of the former transition is 1.2°C in water and 2.5°C in 0.8 M ethanol. For the main transition, the corresponding values are 0.1 and 0.5°C, respectively.

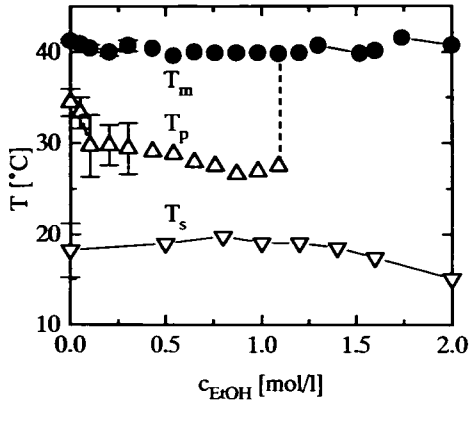

FIGURE 1 Subtransition (▽), Pretransition (△), and chain-melting phase transition temperature (●) of the dipalmitoylphosphatidylcholine multibilayers as a function of the bulk ethanol concentration. Typical error bars are shown for the first four values only.

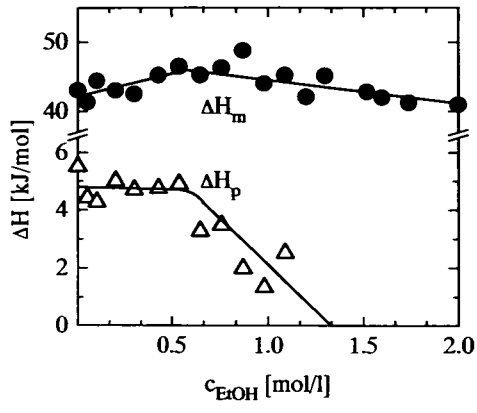

FIGURE 2 Enthalpy of the pretransition (△) and of the chain-melting phase transition (●) of DPPC-suspensions as a function of the bulk ethanol concentration.

X-ray diffraction

To check whether our DSC-based phase assignments are correct, we have studied the DPPC multilayers in various ethanol solutions by means of x-ray small-angle diffraction. By doing so, we have also wanted to investigate the effects of the ethanol binding to the lipid bilayer structures at different temperatures.

Significant changes in the x-ray diffraction patterns were always detected at such temperatures and for such ethanol concentrations that were known to correspond to the transitions observed independently by DSC. Our x-ray measurements, moreover, have proven the coexistence of two lipid lamellar phases below the chain-melting phase transition in 0.7–1.2 M ethanol solutions, which is not detectable by DSC alone. After having assigned appropriate diffraction patterns to both such lipid phases (see further discussion), we have constructed, furthermore, a phase diagram of DPPC in the presence of ethanol (cf. Fig. 3). The corresponding electron density profiles and the molecular packing scheme are illustrated in Fig. 4.

Diffraction patterns in the observed phase regions are as follows:

L_c-phase: After an equilibration at 4°C for 12 days and below the subtransition temperature (between 16 and 18°C), the DPPC samples give rise to at least four reflections with spacings in the ratios 1:0.5:0.33 · · · (see Fig. 5). They were measured for c_{EtOH} = 0, 1.3, 1.6, and 2.0 M and are characteristic of the L_c-phases corresponding to a lamellar repeat distance of (6.30 ± 0.05) nm in pure water and (6.24 ± 0.05) nm in 2.0 M aqueous ethanol. Above 18°C, only the characteristic reflexes of $L_{\beta'}/L_{\beta i'}$-mixtures or of the pure $L_{\beta i'}$-phase were seen (Fig. 6).

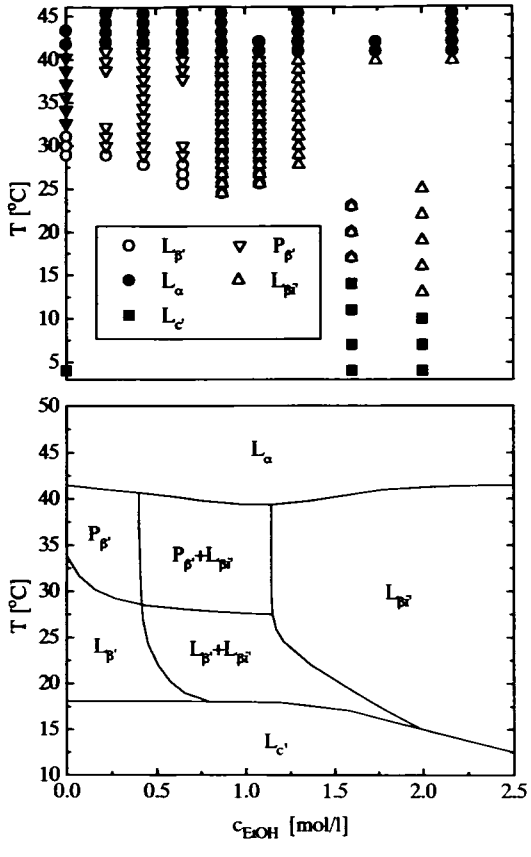

FIGURE 3 Phase diagram of DPPC in various water-ethanol mixtures. (*top*) Experimental x-ray diffraction data. (*bottom*) Phase diagram, based on the combination of calorimetric, fluorescence, dynamic light scattering, and x-ray diffraction data.

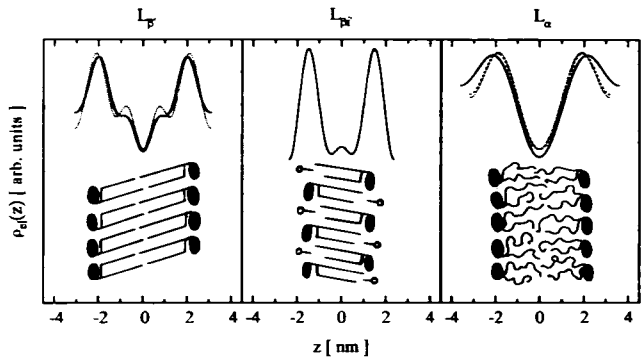

FIGURE 4 Representative electron density profiles derived from the x-ray data measured with DPPC suspensions in 0.3 and 1.6 M ethanol solutions at 22 and 42°C, respectively.

$L_{\beta'}$-phase: At temperatures below the lipid pretransition (i.e., in the $L_{\beta'}$ phase), the hydrated DPPC samples give rise to several sharp low angle x-ray reflections. These correspond to the scattering planes with distances in the ratios of 1:0.5:0.33 · · · (Fig. 6 *c*; on the original films, up to four or five reflections are seen). These peaks are easily identified as the 1st-, 2nd-, 3rd- order Bragg-reflection from the lamellar DPPC structures with a repeat distance of (6.27 ± 0.06) nm.

In the wide angle region, two-component reflections are seen: these consist of one sharp reflection at 0.42 nm, overlapped by a broad reflection centered at 0.41 nm (see also Fig. 6). These peaks correspond to the 10 and 01 reflections of the lateral two-dimensional "distorted hexagonal" lattice of the hydrocarbon chains (Tardieu and Luzzati, 1973). The reason for different widths of these reflections is the different tilt angle of the hydrocarbon chains in both principal directions of the lateral lattice, increasing tilt widening the corresponding reflex (Tardieu and Luzzati, 1973).

$P_{\beta'}$-phase: At any temperature between the lipid pretransition and the chain-melting phase transition, only two low angle x-ray reflections are seen. The second one looks more like a step than like a peak. This is a fingerprint of the undulated lipid multibilayers (Stamatoff et al., 1982). The repeat distance of this phase is (6.71 ± 0.15) nm. In the wide angle region, only one broad reflection at 0.42 nm is seen. This stems from the x-ray scattering on the undistorted hexagonal lattice of the hydrocarbon chains (Tardieu and Luzzati, 1973).

$L_{\beta i'}$-phase: Ethanol concentrations lower than ~0.7 M do not affect the x-ray diffraction patterns of DPPC multibilayers qualitatively. They only shift the lamellar repeat dis-

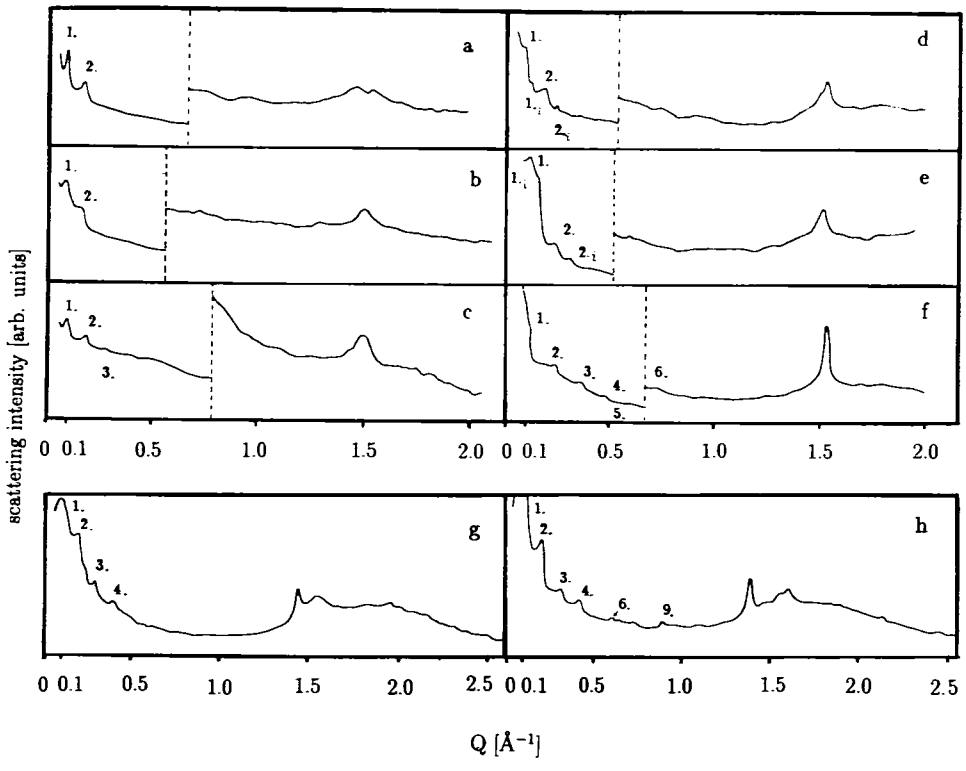

FIGURE 5 Characteristic x-ray diffractograms of DPPC suspensions in the ethanol/water mixtures of various compositions. On the left side, the results of measurements in pure water at $T > T_m$, (L_α-phase) (*a*), $T_m > T > T_p$ ($P_{\beta'}$-phase) (*b*), and $T_p > T$ ($L_{\beta'}$-phase) (*c*) are shown; on the right side, the results of measurements in such water-ethanol solutions that give rise to mixed $L_{\beta'}/L_{\beta i'}$ phases (*d*), to the mixtures of $P_{\beta'}/L_{\beta i'}$ phases (*e*), and to the fully interdigitated phase $L_{\beta i'}$ (*f*) are shown. The bottom panel shows the results of measurements in pure water (*g*) and in 4.13 M EtOH at 4°C. Reflections resulting from the imperfect beamstop, determined in a control experiment without the lipid sample, have been eliminated in the dotted sections.

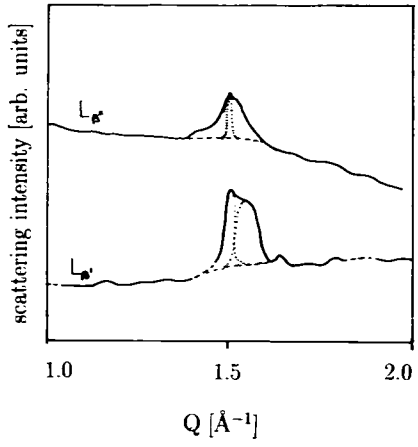

FIGURE 6 Wide angle x-ray reflection measured with DPPC suspensions in pure water (*top*) and in a 0.22 M aqueous ethanol solution (*bottom*) at 29°C.

tance of the $L_{\beta'}$ phase from 6.3 to 6.1 nm with increasing ethanol concentration. In agreement with our DSC measurements we see, however, that the pretransition temperature decreases with increasing ethanol concentration: from a value of 34°C in water, it shifts to 28°C in 0.9 M aqueous ethanol. The chain-melting phase transition temperature of DPPC is also lowered approximately by 1°C in the presence of ethanol (see also Rowe, 1983, 1985).

Ethanol concentrations higher than ~0.7 M give rise to additional x-ray reflections that are not observed in the $L_{\beta'}$- and $P_{\beta'}$-phase. Above 1.2 M ethanol, only these new reflections are seen. All of these are very sharp and diagnostic of the interdigitated lipid lamellae with a repeat distance of (4.88 ± 0.05) nm ($L_{\beta'}$ phase). The coexistence of characteristic reflections from the $L_{\beta i'}$-phase with those from the $L_{\beta'}$- and $P_{\beta'}$-phase, respectively, are a proof for the phase separation in the ethanol concentration region between 0.7 and 1.2 M.

Another remarkable feature of the interdigitated $L_{\beta i'}$-phase observed near the "limiting interdigitation-inducing EtOH concentration" is the very sharp and intensive wide angle reflection at 0.42 nm. This reflection arises from the undistorted hexagonal lateral lattice of the hydrocarbon chains. At high ethanol concentrations, this wide angle reflection splits into a two-component peak, indicative of the distortion of the hexagonal lattice caused by the chain tilting (see further discussion).

L_α-phase: Above the chain-melting phase transition temperature, two very sharp and intense reflections are always observed. They are indicative of the lamellar L_α-phase with a repeat distance of (6.75 ± 0.11) nm. The high angle reflection at 0.46 nm is very broad and much weaker than in the gel-phase; this is a sign of the increased lateral disorder in the molten hydrocarbon chain region.

Thermal expansivity measurements

From the temperature dependence of the wide angle reflections measured with DPPC/water/ethanol mixtures, we were able to calculate the thermal expansion coefficient perpendicular to hydrocarbon chains. From the temperature dependence of the lamellar repeat distance, the thermal expansion coefficient perpendicular to the lamellar planes was deduced.

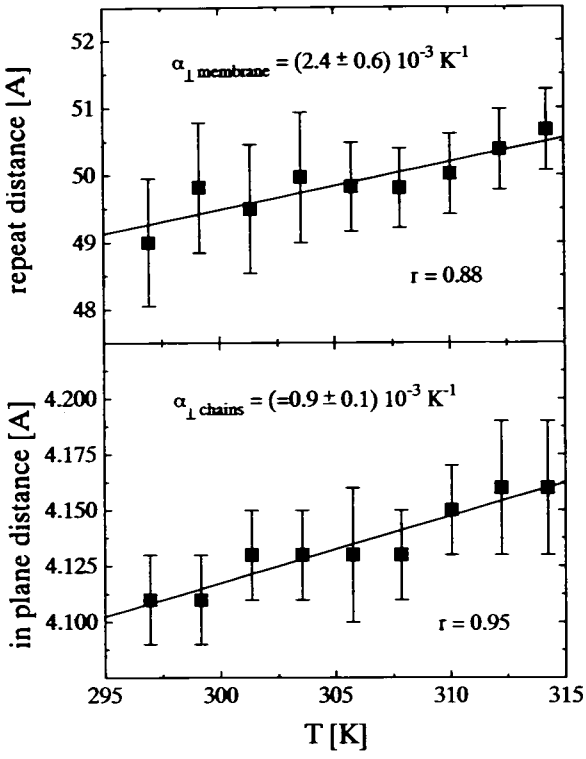

FIGURE 7 Thermal expansion coefficient perpendicular to the lipid chains (*right*) and perpendicular to the lipid lamellae (*left*).

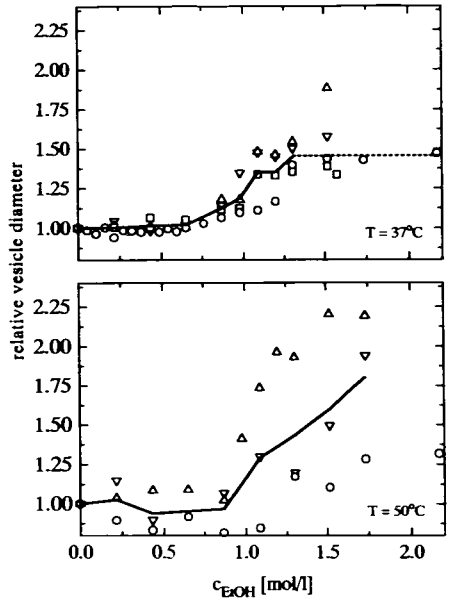

FIGURE 8 Relative diameter of small unilamellar DPPC vesicles as a function of the bulk ethanol concentration in the $P_{\beta'}$-phase at 37°C (*top*) and in the L_α-phase at 50°C (*bottom*). Lines correspond to the mean value of relative vesicle size, as determined in several independent DLS experiments.

For the samples in the interdigitated region (4.3 mol/L EtOH of Fig. 7), we have thus obtained $(0.9 \pm 0.1)\cdot 10^{-3}\ K^{-1}$ and $(2.5 \pm 0.6)\cdot 10^{-3}\ K^{-1}$, respectively.

Dynamic light scattering

In a previous paper, we have reported our results on the ethanol-dependent size variation of unilamellar DPPC-vesicles during the isothermal phase transition from the $L_{\beta'}$- into the $L_{\beta i}$-phase at 25°C (Nagel et al., 1992). Here, we extend such measurements to the temperatures corresponding to the initial existence of the $P_{\beta'}$-phase (37°C) and the L_α-phase 50°C):

$P_{\beta'}$-phase: The results of our size measurements in the undulated $P_{\beta'}$-phase are illustrated in Fig. 8 (*top*). For the bulk ethanol concentrations below 0.6 M, they suggest that the observed vesicle diameter is apparently independent of the bulk ethanol content. This could be because of the diminishment of the optically measurable vesicle size by the bilayer undulations, very similar in its nature to that observed in the $L_{\beta'}$-phase (Nagel et al., 1992).

In the concentration range between 0.6 and 1.0 M EtOH, the diameter of DPPC vesicles increases linearly to 130% of the initial size (cf. Fig. 3).[1] This change is followed by a much steeper size increase in the ethanol concentration range between 1.0 to 1.3 M, which is by 200%. The final vesicle area is again greater by a factor of ≈2—and the final vesicle diameter is greater by a factor of $\approx \sqrt{2}$—than in pure water. This is suggestive of complete lipid-chain interdigitation. Undulated bilayer phases in DPPC bilayers cease to exist for the bulk ethanol concentrations higher than 1.3 M, which precludes measurements in more concentrated EtOH.

L_α-phase: The ethanol-induced variability of the vesicle size in the liquid lamellar, L_α-phase differs from that in the gel-phase. Lines in Fig. 3 (*bottom*) illustrate this, for example, by giving the average vesicle size as a function of the bulk ethanol concentration. Liposome size is here seen to be nearly independent of the bulk ethanol concentration in the concentration range <0.9 M EtOH. Above ~1 M EtOH, however, the average vesicle size increases linearly with the bulk alcohol concentration. Variability of experimental data as well as the sample polydispersity get higher in this EtOH concentration range.

DISCUSSION

Effects of EtOH on the phase behavior of DPPC

As described in our previous paper (Nagel et al., 1992), the addition of ethanol to the DPPC vesicles in the ordered gel phase ($L_{\beta'}$) induces a series of structural transformations that culminate in complete hydrocarbon interdigitation. Most, if not all, of these transformations are caused by the interaction of the alcohol molecules with the polar region of the lipid bilayer. Their most eminent initial manifestation is the hydrocarbon tilt variability. Precise sequence of the events involved in the phosphatidylcholine interdigitation is as follows.

[1] Upper panel in this figure also gives a feeling for the reproducibility of our measurements in the undulated phase. Rectangular symbols give the results obtained with sonicated vesicles. Spherical symbols pertain to the extruded liposomes.

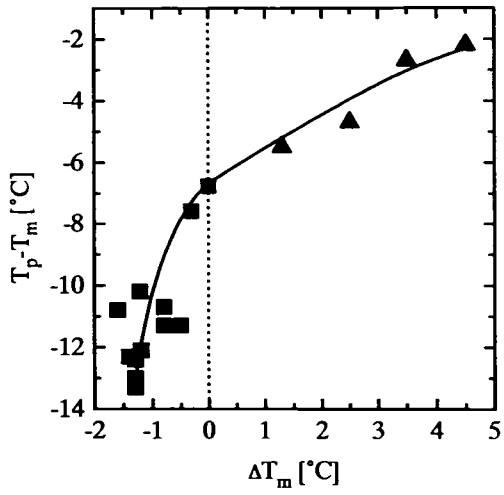

FIGURE 9 The interdependence of the pretransition and the chain-melting phase transition temperature shifts for DPPC vesicles in various aqueous solutions. The positive ΔT_m values were measured with sodium chloride solutions (data from Cevc, 1991c, 1991); the negative values pertain to the water-ethanol mixtures.

The first ethanol molecules that bind to a phosphatidylcholine bilayer start to increase the area per lipid molecule in the interfacial region from 0.48 nm^2 in pure water (Wiener et al., 1989) to 0.67 nm^2 in 0.4 M ethanol (Fig. 10). This effect is balanced by a concomitant increase of the tilt angle θ, which decreases the lipid layer thickness d_t. The chain tilt θ, according to published data, is approx. 30° in pure water (Wiener et al., 1989) and approx. 53° in 0.4 M ethanol (Nagel et al., 1992). This is close to the maximum possible tilt angle of a lipid in the pure $L_{\beta'}$-phase: 55° (Pascher et al., 1981). Values are calculated by the equation:

$$\theta = \arccos\left(\left(\frac{r_{v0}}{r_v}\right)^2 \cos 30°\right).$$

Here r_v is the vesicle-radius, measured by DLS, r_{v0} is the initial vesicle radius, and the initial tilt angle is set to a value of 30° (from Wiener et al., 1989).

Bulk ethanol concentrations higher than 0.4 M thus cannot increase the hydrocarbon tilt angle any further. Lipid bilayers in the highly concentrated ethanol solutions, consequently, proceed to increase their interfacial area by another mechanism: the lipid chain interdigitation. The reason for this is that the molecular area in any fully interdigitated phase is by a factor of about two greater than in the corresponding non-interdigitated phase.

X-ray diffraction results were published before for isolated points in the phase diagram of DPPC. These data have proven that DPPC forms an interdigitated gel $L_{\beta i'}$-phase in the presence of ethanol and other drugs or ions (McIntosh et al., 1983; Simon and McIntosh, 1984). In Rowe (1983), the minimum ethanol concentration needed to induce a complete chain interdigitation was estimated to be 1.1 M.

Our measurements confirm the existence of an interdigitated gel phase with a repeat distance of 4.9 nm. Moreover, they reveal, that below 1.2 M, only a part of the membrane

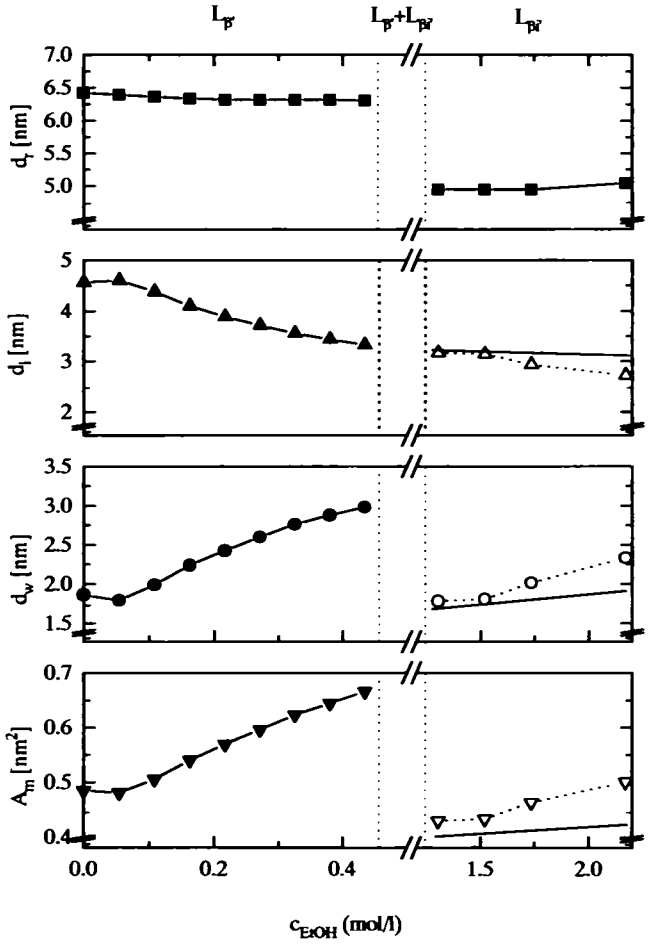

FIGURE 10 Structural parameters of the $L_{\beta'}$-phase DPPC multi-bilayers in water-ethanol solutions as a function of the bulk ethanol concentration. Membrane thickness d_t from the dynamic light-scattering measurements with extruded small unilamellar vesicles; repeat distance from x-ray data. Because of the partial aggregation of small unilamellar vesicles in the $L_{\beta i}$-phase while the DLS-measurement, the values of the membrane thickness in the interdigitated phase are systematically too low and the decrease is overestimated (*open symbols*). The extrapolation of the x-ray data gives a tilt angle of ~10° at 4 M EtOH. This suggests values shown as line.

is interdigitated. The coexistence of characteristic x-ray reflections from the $L_{\beta i}$ with the $L_{\beta'}$ and the $P_{\beta'}$-phase, respectively, verifies this fact. Above the limiting ethanol concentration of 1.2 M, the "bilayer" consists of a pure $L_{\beta i}$-phase.

Minimum ethanol concentration needed for the induction of the hydrocarbon interdigitation, as evaluated from the small angle x-ray diffraction experiments, is higher than that determined by means of the dynamic light scattering. This is in apparent conflict with the results of the recently published fluorescence measurements (Boni et al., 1993). These measurements suggest that the curvature stress in a small vesicle, as used in our DLS measurements, should increase the minimal ethanol concentration needed to induce complete chain interdigitation. This discrepancy could be an artifact, however, caused by the fact that the reflections from the interdigitated phase are weaker than those from the ordinary lipid bilayers. In the early stages of chain interdigitation, the former reflections could thus be hidden behind the

reflections from the noninterdigitated lipid bilayers, or by the background scattering.

Wide angle reflections reveal that the area per lipid chain, within the accuracy of our measurements, is the same for all investigated ethanol/water mixtures. A value of 0.23 nm^2 per chain, for example, is calculated from the data of Fig. 6. This justifies the incompressibility assumption made in the evaluation of the dynamic light scattering data. The specific volume of each lipid molecule, which is chiefly determined by the chain-packing characteristics, is thus well conserved.

To estimate the hydrocarbon tilt in the interdigitated phase, we have also determined the bilayer repeat distance by means of the x-ray small angle diffraction as a function of PC chain length. Data analysis has proven that DSPC and DAPC have a very similar phase diagram as DPPC, with extensive regions of coexistence between the interdigitated and non-interdigitated state. The previously published phase diagrams for these lipids in aqueous ethanol (Rowe and Cutrera, 1987; Nambi et al., 1988) should be corrected correspondingly.

The measured lamellar repeat distance 10°C below the chain-melting phase transition temperature on the fringe of full interdigitation and deep in the $L_{\beta i}$-region is shown in Fig. 11 as a function of the chain length. This suggest the following conclusions. First, the hydrocarbon tilt in the interdigitated phase at the onset of complete interdigitation is zero. This can be seen, on the one hand, from the measured repeat distance increment, which is (0.130 ± 0.005) nm per CH_2-group. Within the experimental error, this equals the length of an untilted CH_2 group. On the other hand, the very sharp one-component wide-angle peak also provides evidence for the undistorted hexagonal lattice, characteristic of zero tilt.

Far beyond the critical ethanol concentration, however, the situation changes. The hydrocarbon chains are now tilted in the interdigitated phase. This can be seen from the decrease

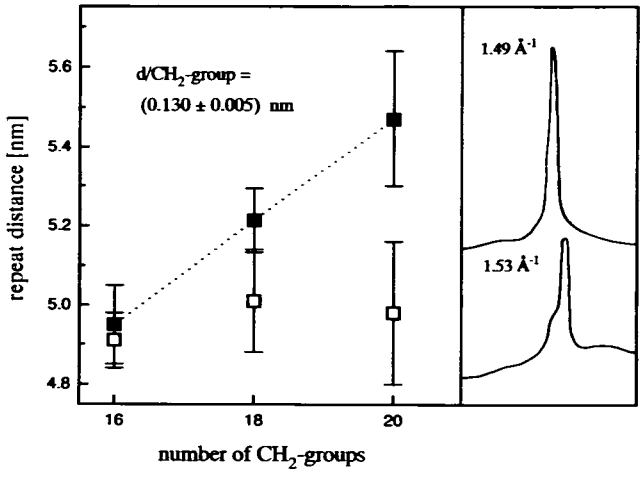

FIGURE 11 (*left*) Repeat distance 10°C below the main transition temperature at ethanol concentrations corresponding to the onset of complete membrane interdigitation (■, C_{EtOH} = 0.5, 0.9, 1.3 M) and far beyond the critical concentration (□, C_{EtOH} = 4 M) as a function of the hydrocarbon chain length. (*right*) Wide angle reflection of DSPC at 0.9 M EtOH (*above*) and at 4 M EtOH.

of the repeat distance of (0.011 ± 0.006) and (0.013 ± 0.008) nm per CH_2-group for DSPC and DAPC, respectively. The splitting of the wide angle reflection into a sharp and a broad component (Fig. 11) also speaks in favor of such an assignment. The latter results from the distortion of the hexagonal lattice of hydrocarbon chains, tilted in one basic direction of this lattice (Tardieu and Luzzati, 1973).

Taking the water layer thickness d_w to be approximately 2 nm (cf. Fig. 5), the chain tilt, in the first approximation, is given by $\theta = \arccos(d_r - d_w/d_{r0} - d_w)$, d_r being the repeat distance and d_{r0} the repeat distance at zero tilt. At 4 M ethanol, the tilt angles thus calculated for DSPC and DAPC are (20 ± 7)° and (30.8 ± 7)°. Taken that PCs with longer chains are more sensitive to the alcohol binding (Rowe, 1983), such a difference is to be expected. This also suggests that our previous conclusion that DPPC directly forms an interdigitated phase with tilted chains (Nagel et al., 1992) was incorrect. The reason for this error might be the irreversible aggregation of very small unilamellar interdigitated vesicles (Boni et al., 1993; Komatsu et al., 1993) used in our previous study. This has probably led to an overestimation of the vesicle radius in the interdigitated phase region and has resulted in a systematic error in the calculated chain tilt. In this study, all DLS measurements entering in the calculation of the tilt angle in the $L_{\beta'}$-phase were done with extruded small unilamellar vesicles (diameter ~100 nm), which are stable against the aggregation in the $L_{\beta'}$-phase (Komatsu et al., 1993). The constant polydispersity data (not shown) throughout the experiments confirms this assumption.

The mechanism of chain interdigitation starting from the $P_{\beta'}$-phase is almost the same. X-ray diffraction data reveal (see Fig. 5 *b*) that the "linear increase" of the DPPC vesicle size measured for the aqueous ethanol solutions with concentrations between 0.6 and 1.2 M EtOH at 37°C is representative of a two-phase region in which the $P_{\beta'}$- and $L_{\beta'}$-phases coexist. This suggests that the corresponding structural changes in the former phase proceed in very much the same way as in the $L_{\beta'}$-phase. This is to say that a continuous bilayer transformation from the undulated membranes into fully interdigitated planar (but thermally fluctuating) bilayers is likely to occur.

Bilayer surface undulations affect the measurable vesicle size. Direct monitoring of the variability of hydrocarbon tilt by means of the dynamic light scattering or a similar determination of the degree of chain interdigitation in the phase coexistence region is thus not possible.

A different situation is found above the chain-melting phase transition temperature. Here, the increase of the DPPC vesicle size caused by ethanol concentrations higher than 0.9 M is not caused by lipid chain interdigitation. Based on our x-ray diffraction data and molecular reasoning, one can even argue that above the chain-melting phase transition temperature no chain interdigitation should occur, for the symmetric-chain phospholipids at least. Any area expansion of such lipids can namely be achieved simply by an extra extension in the lateral direction and needs not to involve any chain

interdigitation. The increased average size of the phosphatidylcholine vesicles in the fluid lamellar phase in the presence of ethanol, therefore, is not indicative of such a chain interdigitation. Rather, it is probably caused by the intervesicle aggregation and/or fusion (Boni et al., 1993; Komatsu et al., 1993). The observed increase in the vesicle suspension polydispersity, which is also reflected in the increased experimental scatter, corroborates this conclusion (cf. Fig. 3).

Vesicle size, as a function of the bulk ethanol concentration, begins to increase rapidly for alcohol concentrations giving rise to more than 50% interdigitation below the chain-melting phase transition temperature (>0.9 M EtOH). The propensity for the hydrocarbon interdigitation at $T < T_m$ thus coincides with the catalysis of the intervesicle aggregation/fusion above this transition temperature.

Thermodynamic properties

We have combined the results of our DSC-, DLS-, and x-ray diffraction measurements to create a new and more complete phase diagram for the fully hydrated DPPC in the presence of ethanol. We have also devised a rather complete picture of the structural, solvation, and phase characteristics of such systems.

At relatively low temperatures, all phospholipids form crystalline phases. In its prevailing hydrated crystal $L_{c'}$-form DPPC has a "hydration shell" of some 11 water molecules (Ruocco and Shipley, 1982). The tightly packed lipid chains are then located on an orthorhomic lattice (Ruocco and Shipley, 1982; Mulukutla and Shipley, 1984). Upon heating above $T \geq T_\beta = 18°C$, DPPC undergoes a transition from the $L_{c'}$ into a $L_{\beta'}$-phase (Fūldner, 1981). This characteristic subtransition temperature appears to be nearly insensitive to the solvent composition or the chain-terminus, i.e., to the type and/or the state of the polar lipid headgroup (Finegold and Singer, 1986; Lewis et al., 1987). (For the ideally packed C_{16}-alkane, the subtransition temperature is 4°C (Cevc, 1991c, 1991). The fact that ethanol concentrations above 1.2 M lower the subtransition temperature of DPPC to ~15°C (without affecting the subtransition enthalpy) is thus quite significant. Together with the results of our x-ray diffraction measurements, it shows that the packing of the hydrocarbon chains in interdigitated DPPC layers is only little constrained by the headgroup characteristics and thus more alkane-like.

This highlights the mechanism by which ethanol facilitates the crystallization of lipid molecules in aqueous suspensions. It also explains why the undercooled $L_{\beta'}$-phase is less stable in the presence of EtOH and finally vanishes in the highly concentrated alcohol solutions. The molecular basis of all these phenomena is the elimination of the steric constraints in the interfacial region.

The number of water molecules that are rather tightly bound to each phosphatidylcholine headgroup is similar to that in the L_c and $L_{\beta'}$-phase, ~11 (Ruocco and Shipley, 1982; Wiener et al., 1989). This value does not include the surface-perturbed water, however, which may involve another 5–6 H_2O in the latter phase only. Recent FTIR studies (Chiou et al., 1992) have shown ethanol to replace some of the water bound to the DPPC headgroups. According to these measurements, the phosphate group is the primary binding site for the ethanol molecules. Based on the ^{2}H-NMR order parameter profiles of the alcohol molecules in other lipid systems (Jonströmer and Strey, 1993), and by logical reasoning, we expect that the OH-residues on ethanol are hydrogen-bonded to one of the oxygens of the phosphate group, whereas alkyl-chains insert themselves in the interfacial region so as to point towards the hydrocarbon interior. Ethanol location near, or slightly deeper than, the phosphate group is also expected from the comparison of local polarities (or dielectric constants). They are ~30 at the level of phosphate groups (Cevc et al., 1981) and 24 in pure ethanol (Weast and Astle, 1986).

Lipid pretransition speeds up the rotation of lipid headgroups around the P-O-bonds (Fūldner, 1981). According to the ^{31}P-NMR measurements with DMPC (Dufourc et al., 1992), a $P_{\beta'}$-phase is an intermediate between the gel-phase and the liquid-crystalline phase. The ordinary order parameter S_{xx}, as well as the tilt angle with respect to the bilayer plane, both split in two components, typical for the two neighboring phases. In addition to this, so-called restricted rotational diffusion of the lipid molecule as a whole is observed (Blume, 1993). Simultaneously, the hydration of lipid headgroups increases appreciably (Parsegian, 1983). These increases have been claimed to induce lipid pretransition (Cevc, 1991c, 1991) and to give rise to the bilayer surface undulations, which are diagnostic of the $P_{\beta'}$-phase.

Upon the transition into a $P_{\beta'}$-phase, some of the hydration-dependent free energy gain is lost. This is because of the sliding of the hydrocarbon chains and because of the concomitant loss of the inter-chain van der Waals attraction in such an undulated phase. The larger is the absolute value of the hydration free energy of a given lipid, the lower can be the pretransition temperature. The energy supplied by the ethanol binding to the lipid headgroups can improve this energy balance and shift the pretransition temperature downwards. In such a picture, the enthalpy of the lipid pretransition should remain approximately the same, however, because little or no extra disorder in the lipid bilayers is created by the ethanol binding.

This is precisely what we observe. The pretransition enthalpy is essentially the same, 5 kJ mol^{-1}, for all investigated ethanol concentrations. The shift of the pretransition temperature is nonlinearly proportional to the shift of the chain-melting phase transition temperature, as has been reported before (Cevc, 1991c, 1991). Fig. 9 documents this for DPPC in sodium chloride and ethanol solutions, respectively.

The onset of the hydrocarbon interdigitation in $c_{EtOH} \geq 0.4$ M modifies this picture. Creation of the interdigitated domains in lipid bilayers, as measured directly by means of the small angle x-ray diffractometry, decreases the enthalpy of the lipid pretransition, as measured by DSC. This decrease appears to be directly proportional to the occurrence of $L_{\beta i}$-domains in the investigated system (cf. Fig. 2 and 3). This is because, according to Gibbs' phase rule, interdigitated domains do not participate in the lipid pretransition. In contrast to former publications (Nambi et al., 1988; Ohki et al., 1990), our phase diagram thus forbids a direct $L_{\beta'} \rightarrow L_{\beta i}$ transition.

Pretransition enthalpy should consequently decrease with the progress of hydrocarbon on interdigitation until, in a 1.2 M ethanol solution, the chain interdigitation can be complete. By then, the pretransition enthalpy has decreased to zero.

The chain-melting phase transition temperature of dipalmitoylphosphatidylcholine in the presence of ethanol mirrors the relative affinity of such alcohol molecules for the lipid phases involved. Nambi et al. (1988) have pointed out that the relative attractivity of various phosphatidylcholine phases to the ethanol molecules increases in the sequence $P_{\beta'} < L_\alpha < L_{\beta i}$. This decreases the chain-melting phase transition temperature of PCs in relatively dilute ethanol solutions and increases T_m values of the interdigitated hydrocarbon chains. We believe that ethanol concentrations exceeding 0.4 M give rise to the domains of interdigitated hydrocarbon chains.

The solvent-induced shift of the chain-melting phase transition temperature, to a good approximation, is proportional to the solvation free energy change at this phase transition (Cevc and Marsh, 1985):

$$\Delta T_{m,h} = N_A \Delta F_{m,h}(A_l)/\Delta S_{m,ref}.$$

$\Delta S_{m,ref}$ is the transition entropy of a mole of lipids in the reference state, N_A is Avogadro's number, and A_l is the molecular area per lipid. (If one is only interested in relative numbers, the value of $\Delta S_{m,ref}$ can be taken to be identical to the chain-melting phase transition entropy of lipids in pure water.)

From the data shown in Fig. 1, we conclude that the solvation free energy of bilayers decreases at $T = T_m$. The hydration energy of lipids in pure water and in the ethanol-water mixtures ($F_h(A_l)$) is probably rather similar; the smallness of the alcohol-induced shift of the chain-melting phase transition temperature suggests this. The absolute value of this free energy is doubtlessly quite high, however, as concluded from the large number of the headgroup-bound solvent molecules (see next section).

Alternatively, one can calculate the chain-melting phase transition temperature of PC from the phenomenological expression (Cevc, 1991b):

$$T_m(n_C) = 400\,(1 - 1.347/n_C - 18.842/n_C^2)\ K,$$

where n_C corresponds to an effective hydrocarbon chain-length. For the systems with untilted chains, this value is identical to the nominal length of the acyl chains. When the transition involves a low temperature phase with tilted chains, however, one should use $n_C = n_{C,nominal} \cos\theta$ (Cevc 1991b). With this in mind, one immediately finds the relation between the relative molecular area of lipids with untilted and tilted chains, $A_l/A_{0l} = \cos\theta$ and the T_m value. For DPPC, one gets approximately

$$T_m \sim 400\,[1 - 0.1125 \cdot (A_l/A_{0l}) - 0.0984 \cdot (A_l/A_{0l})^2]\ K$$

A_{l0} being $\sim$0.42 nm^2. This explains why the chain-melting phase transition temperature of fully hydrated lipids always gets smaller when the area per molecule increases (cf. Fig. 1 and 10). (This latter expression is not very accurate, however, because of the neglect of the higher order terms and other corrections.)

The enthalpy of any first order phase transition is directly proportional to the entropy change during such phase transition. Ethanol binding is likely to disorder part of the lipid headgroup region. Following the same line of reasoning as before, we now argue that the entropy change associated with the transition from a $P_{\beta'}$- into the L_α-phase should be lower than in the case of a $L_{\beta i} \rightarrow L_\alpha$ transition. Our measurements confirm this trend. They moreover show that the enthalpy of the lipid chain-melting phase transition decreases with increasing bulk ethanol concentration for $c_{EtOH} \geq 0.4$ M.

Effects of ethanol on the packing properties of DPPC molecules

Water binding to the polar lipid heads causes lipid bilayers to swell in all directions. This swelling, in the first approximation, can be taken to be proportional to the lateral and transverse pressures on each lipid molecule.

For an anisotropic system, such as a lipid bilayer, the change in the area per lipid can be taken to be proportional to the change in the lateral pressure of hydration, Π_h, (Cevc and Seddon, 1986).

$$\Delta A_l \simeq \frac{|\Delta\Pi_h(d_w)|}{K_A},$$

K_A being the membrane compressibility modulus. Lateral pressure of hydration is given by the surface derivative of bilayer free energy of hydration:

$$\Pi_h(d_w, \sigma_p) = \partial F_h(d_w, \sigma_p(A_l))/\partial A_l,$$

where the local excess charge density, $\sigma_p(A_l)$, gives the measure for the surface hydrophilicity.

Likewise, the repulsive pressure between lipid bilayers (so-called hydration force) is given by

$$p_h(d_w, \sigma_p) = \partial F_h(d_w, \sigma_p(A_l))/\partial d_w.$$

By comparing the ethanol-induced phase transition shift data (cf. Fig. 1) with the ethanol-induced area increase of (cf. Fig. 8), we conclude that these two phenomena are closely related. This is also reflected in the shift interdependence illustrated in Fig. 9.

It is highly probable that the increased SD of our dynamic light scattering results in the interdigitated phase is caused by the much greater fluctuations of the lipid vesicle membranes in such a phase. This is mainly caused by the decreased membrane bending modulus; the reduced membrane thickness as well as the changing interlipid interactions, and the lack of inter-layer packing, can all contribute to this. The much stronger membrane fluctuations in the interdigitated phase are also possible for the multilamellar systems. In such systems, moreover, the fluctuation-driven repulsion between the lipid membranes can increase the interlamellar water thickness, as has been reported by Safinya and his colleagues

for the dimyristoylphosphatidylcholine/pentanol/water and some other alcohol/water mixtures (Safinya et al., 1988).

In contrast to previous authors, we do not expect membrane thickness to change with the alcohol chain length in a monotonous manner. We anticipate that only the short- but not the long-chain alcohols induce chain interdigitation, octanol being the limiting case between the two regimen (L. Löbbecke and G. Cevc, unpublished data). Such a switch can also explain the kink in the published rigidity versus alcohol chain length data (Safinya et al., 1988).

It has previously been suggested that water layer thickness in certain interdigitated phosphatidylcholine/organic solvent mixtures can be as big as 20 nm (Safinya et al., 1988). Swelling like this would cause some of the suspensions used in x-ray diffraction experiments to be incompletely hydrated, because of the high lipid concentration. To exclude that this has happened, we have repeated some of the measurements with samples with a 5 times lower lipid concentration (data not shown). No additional swelling was observed, however. This proves that all systems investigated in this work were under excess-solvent conditions.

Colloidal properties of the interdigitated lipid systems

The decrease of the lamellar repeat distance in the $L_{\beta'}$-phase of DPPC multibilayers is mainly a consequence of the increased chain tilt. To determine the effects of ethanol molecules on the colloidal behavior of PC, and to extract the information about the effective hydration of this lipid, we have thus combined the lamellar repeat distances measured with x-ray diffraction with the bilayer thickness data determined from the dynamic light scattering measurements data (from Nagel et al., 1992). This was made under the assumption that lipid layer thickness is the same in the unilamellar and the multilamellar systems.

Repeat distance, as measured by means of the small-angle x-ray diffraction, is the sum of the lipid bilayer thickness, d_l, and interlamellar water layer thickness, d_w. If the former is known, the latter can thus be calculated from

$$d_w = d_r - d_l.$$

The results of the corresponding calculations are shown in Fig. 8. They indicate that the bulk ethanol concentration only moderately affects the bilayer repeat distance. In contrast to this, it affects the calculated bilayer thickness quite strongly. The resulting decrease is caused by the alcohol dependence of the hydrocarbon tilt (cf. Fig. 10). Water layer thickness in the pure $L_{\beta'}$-phase of DPPC thus increases by approximately 75% to 3.0 nm ($c_{EtOH} \leq 0.5$ M). (This latter value is even greater than that measured with DPPC in the fluid lamellar phase, for which we find $d_w \simeq 2.8$ nm). In volume terms, the ethanol-induced swelling is even more pronounced, being given by the product of the increased area per lipid molecule times the increased water layer thickness. The ethanol-induced increase in the "bound water" volume amounts to ~130%. This corresponds to more than 50 water molecules. The increase is greater by at least a factor of two in the interdigitated phase.

The equilibrium interbilayer separation corresponds to the state of zero total force between lipid membranes, or nearly so (Cevc and Marsh, 1987). For the uncharged lipids this condition can be written as

$$p_{vdW} - p_h - p_f \approx 0, \tag{1}$$

where p_{vdW} gives the van der Waals, p_h the hydration, and p_f the fluctuation-dependent contribution to the total pressure in the system. The dependence of interbilayer separation, d_w, on these contributions is approximately given by (see Cevc and Marsh, 1987)

$$p_{vdW}(d_w) \approx \frac{H_A}{6\pi}\left[\frac{1}{d_w^3} - \frac{2}{(d_l + d_w)^3} + \frac{1}{(2d_l + d_w)^3}\right] \tag{2}$$

$$p_h(d_w) \approx p_0 \cdot \exp\left(\frac{d_w}{\Lambda}\right) \tag{3}$$

$$p_f(d_w) \approx \left(\frac{\pi kT}{32}\frac{\partial^2 \sum_i p_i(d_w)}{\partial d_w^2}\right)\left(B\frac{\partial \sum_i p_i(d_w)}{\partial d_w}\right)^{-1/2}, \quad i = vdW, h. \tag{4}$$

The Hamaker constant, H_A, is a function of the dielectric constants of the membrane interior and of the bulk aqueous solution. In the range 0–0.5 M ethanol, the decrease of static dielectric constant is only small, from 81.1 to 79.5. For the present purpose, the value of H_A can thus be approximated by the Hamaker constant pertaining to the lipid suspensions in pure water at comparable temperatures. The corresponding value for $T = 20°C$ has been estimated to be 5.3×10^{-21} $J \simeq H_A$, and measured to be $5–6 \times 10^{-21}$ J, for example.

To fulfill Eq. 1, it is necessary that p_0 and/or Λ changes. To determine these changes, one can insert the measured interbilayer water layer thickness data into Eq. 1. One then gets $\Lambda(c_{EtOH})$ for each given value of H_A. Alternatively, $p_0(c_{EtOH})$ can be calculated by assuming that the other variable is always constant.

Fig. 12 presents the results of such calculations made under the assumption that $\Lambda = 0.12$ nm and $p = p(c_{EtOH})$ or else that $p_0 = 1.5 \cdot 10^{11}$ Nm^{-2} and $\Lambda = \Lambda(c_{EtOH})$l. If Λ is constant, p_0 is concluded to increase by 3 orders of magnitude, which makes no physical sense (see Fig. 12). This suggests that extra interbilayer repulsion caused by the ethanol binding to or insertion into the interfacial region is mainly a result of the longer effective decay length value of interfacial repulsion. The maximum of Λ in 0.43 M ethanol, just before the onset of complete hydrocarbon interdigitation, is calculated to be (0.163 ± 0.009) nm. Binding of the ethanol molecules to the polar lipid headgroups thus increases the lateral pressure in the headgroup region, and it also strengthens the interbilayer repulsion. This can be explained as follows.

In the most recent model of hydration force (Cevc, 1991a; Kirchner, 1993; Hauser, 1993), the interfacial hydration pressure is taken to be a function of the interfacial polarity

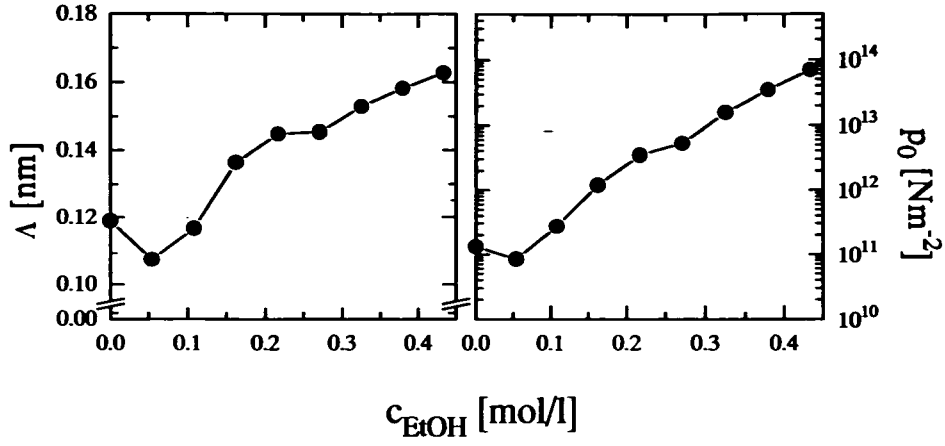

FIGURE 12 Effective decay length of interbilayer repulsion (Λ, *left*) and the extrapolated, maximum surface pressure (p_0, *right*) as a function of the bulk ethanol concentration. All values were calculated from Eqs. 2, 3, and 4 using the data of Fig. 8.

profile, $\rho_p(z)$. The latter describes the distribution of the water binding sites in the interfacial region. Its effect on the hydration pressure modeled in the nonlocal electrostatic approximation can be written as a function of membrane hydration potential, $\Psi_h(z)$:

$$p = -\frac{1}{A_l}\frac{\partial F_h}{\partial d_w} = \frac{1}{2}\frac{\partial}{\partial d_w}\left\{\int_0^{d_w} \rho_p(z, d_w)\Psi_h(z)\, dz\right\}. \qquad (5)$$

This hydration potential, in the linear approximation, is given by the solution to the differential equation

$$\Lambda^2\Psi_h''(z) - \Psi_h(z) = \frac{\Lambda^2}{\epsilon_0\epsilon_\infty(1 - \epsilon_\infty/\epsilon)}\rho_p(z, d_w), \qquad (6)$$

with the boundary condition $\Psi_h'(0) = \Psi_h'(d_w) = 0$. ϵ and $1.8 \le \epsilon_\infty \le 4.6$ are the static and high frequency dielectric constants of the solvating medium and Λ is the corresponding intrinsic value of the solvent correlations decay length. This latter parameter depends on the solvent type and model. For water, Λ-values between 0.07 nm (Cevc, 1991a) and 0.3 nm (Kornyshev and Leikin, 1989) have been suggested. The directly measured, apparent values are typically 0.12 nm in the gel- and around 0.25 nm in the fluid lamellar phase (Rand and Parsegian, 1990). For the short chain alcohols, the apparent solvation decay length is approx. (0.1 ± 0.03) nm (M. Hirth and G. Cevc, unpublished data).

Within the framework of such model, the width of polarity distribution function

$$d_p = \frac{\int z\rho_p(z, d_w)\, dz}{\int \rho_p(z, d_w)\, dz} \qquad (7)$$

starts to affect the range and the strength of interfacial repulsion. In fact, this width can become more important for the range of hydration-dependent pressure than the water correlations decay length itself. This is true at least as soon as the interfacial thickness is much greater than this latter decay length. Many experimental lipid systems, including ours, are likely to fall in this category.

Our theoretical analysis shows (Hauser, 1993; Cevc, 1991a) that interfacial smearing can strongly influence the apparent decay length, Λ_{eff} of the hydration-dependent force between the laterally homogeneous surfaces, representative of the polar phospholipid membranes. For the surfaces with a thick interfacial region, the range of hydration force is dominated by the variable interfacial thickness, d_p/s. By increasing this thickness, e.g., through the addition and binding of ethanol to the lipid headgroups, the decay length of hydration force thus gets longer.

Such increase is indirectly observed in our study (cf. Fig. 12). The increase of the effective decay length of solvation-dependent interbilayer repulsion can thus be explained tentatively by the insertion of the ethanol molecules into the lipid headgroup region. Lipid headgroups, therefore, are likely to be more extended in the $L_{\beta i'}$-phase than in the $L_{\beta'}$-phase. Solvent molecules are then more likely to penetrate deep in the hydrocarbon region. Both of these phenomena should increase the range of solvation-dependent interbilayer repulsion.

In summary, we have shown that ethanol binding to the phospholipid bilayers tends to increase lateral as well as transverse repulsion between the lipid molecules. The former pressure gives rise to an ethanol-dependent change of the area per molecule; the latter leads to excessive swelling of phosphatidylcholine bilayers in the aqueous ethanol solutions. As a result of all this, ethanol can induce hydrocarbon interdigitation and increase intermembrane separation in the gel phase. Ethanol also broadens the interface and, by doing so, increases the range and extent of the lipid headgroup solvation. Lipid pretransition temperature is very sensitive to the addition of ethanol. Even minute amounts of this co-solvent shift the pretransition temperature downwards by up to 10 degrees. In contrast to this, the subtransition (rotator phase transition) as well as the chain-melting phase transition temperature of DPPC are little affected by the presence of ethanol, the corresponding shifts being always smaller than 3 degrees. High alcohol concentrations (>1.2 M) prevent periodic bilayer undulation: this is the generation of $P_{\beta'}$-phase. Interdigitated lipid bilayers thus melt directly into the ordinary fluid-lamellar phase. Above c_{EtOH} = 1.2 M and above the bilayer fluidization temperature lipids are (partly) solubilized by the bound ethanol molecules. In aqueous ethanol with alcohol concentrations higher than 7 M, PC forms mixed micelles with alcohol above the chain-melting phase transition temperature.

This study has been supported financially by the Deutsche Forschungsgemeinschaft through grants Ce 19/2-2 and SFB 266/C8.

REFERENCES

Blaurock, A. E., and C. R. Worthington. 1966. Treatment of low angle x-ray data from planar and concentric multilayered structures. *Biophys. J.* 6:305–312.

Blume, A. 1993. Phospholipids Handbook. G. Cevc, editor, Marcel Dekker, New York.

Boni, L. T., S. R. Minchey, W. R. Perkins, P. L. Ahl, J. L. Slater, M. W. Tate, S. M. Gruner, and A. S. Janoff. 1993. Curvature-dependent induction of the interdigitated gel phase in DPPC vesicles. *Biochim. Biophys. Acta.* 1146:247–257.

Cevc, G., and D. Marsh. 1987. *Phospholipid Bilayers.* John Wiley & Sons, New York.

Cevc, G. 1991. Hydration force and the interfacial structure of the polar surface. *J. Chem. Soc. Faraday Trans.* 87:2733–2739.

Cevc, G., and J. M. Seddon. 1986. Structural and dynamic consequences of amphiphile hydration. *In* Surfactants in Solution. Vol. 4 K. L. Mittal, editor Plenum Press, New York. 243–252.

Cevc, G., A. Watts, and D. Marsh. 1981. Titration of the phase transition of phosphatidylserine bilayer membranes. Effects of pH, surface electrostatics, ion binding, head-group hydration. *Biochemistry.* 20: 4955–4965.

Cevc, G. 1991. How membrane chain-melting phase transition temperature is affected by the lipid chain-asymmetry and degree of unsaturation: analysis and predictions based on the effective chain-length model. *Biochemistry.* 30:7186–7193.

Cevc, G., and D. Marsh. 1985. Hydration of noncharged lipid bilayer membranes theory and experiments with phosphatidylethanolamines. *Biophys. J.* 47:21–31.

Cevc, G. 1991. Polymorphism of bilayer membranes in the ordered phase and the molecular origin of lipid pretransition and rippled lamellae. *Biochim. Biophys. Acta.* 1062:59–69.

Chiou, J.-S., P.-R. Krishna, H. Kamaya, and I. Ueda. 1992. Alcohols dehydrate lipid membranes: a infrared study on hydrogen bonding. *Biochim. Biophy. Acta.* 1110:225–233.

Dufourc, E. J., C. Mayer, J. Stohrer, G. Althoff, and G. Kothe. 1992. Dynamics of phosphate head groups in biomembranes. Comprehensive analysis using phosphorus-31 nuclear magnetic resonance lineshape and relaxation time measurements. *Biophys. J.* 61:42–57.

Finegold, L., and M. A. Singer. 1986. The metastability of saturated phosphatidylcholines depends on the acyl chain length. *Biochim. Biophys. Acta.* 855:417–420.

Fūldner, H. H. 1981. Characterization of a third phase transition in multilamellar dipalmitoyllecithin liposomes. *Biochemistry.* 20:5707–5710.

Jonströmer, M., and R. Strey. 1993. Nonionic bilayers in dilute solutions: the effect of additives. *J. Phys. Chem.* 62:79–90.

Kirchner, S., G. Cevc. 1994. Hydration of polar interfaces. A generalised mean-field model. *J. Chem. Soc. Faraday Trans.* 90:1941–1951.

Komatsu, H., P. T. Guy, and E. S. Rowe. 1993. Effect of unilamellar vesicle size on ethanol-induced interdigitation in dipalmitoylphosphatidylcholine. *Chem. Phys. Lipids.* 65:11–21.

Kornyshev, A. A., and S. Leikin. 1989. Fluctuation theory of hydration forces: the dramatic effects of inhomogeneous boundary conditions. *Phys. Rev. A.* 40:6431–6438.

Lewis, R. N. A., N. Mak, and R. N. McElhaney. 1987. A differential scanning calorimetric study of the thermotropic phase behavior of model membranes composed of phosphatidylcholines containing linear saturated fatty acyl chains. *Biochemistry.* 26:6118–6126.

Lin, H., Z. Wang, and C. Huang. 1991. The influence of acyl chain-length asymmetry on the phase transition parameters of phosphatidylcholine dispersions. *Biochim. Biophys. Acta.* 967:17–28.

Mattai, J., P. K. Sripada, and G. G. Shipley. 1987. Mixed-chain phosphatidylcholine bilayers: structure and properties. *Biochemistry.* 26: 3287–3297.

McDaniel, R. V., T. J. McIntosh, and S. A. Simon. 1983. Nonelectrolyte substitution for water in phosphatidylcholine bilayers. *Biochim. Biophys. Acta.* 731:97–108.

McIntosh, T. J., A. D. Magid, and S. A. Simon. 1989. Range of the solvation pressure between lipid membranes: dependence on the packing density of solvent molecules. *Biochemistry.* 28:7904–7912.

McIntosh, T. J., R. V. McDaniel, and S. A. Simon. 1983. Induction of an interdigitated gel phase in fully hydrated phosphatidylcholine bilayers. *Biochim. Biophys. Acta.* 731:109–114.

Mulukutla, S., and G. G. Shipley. 1984. Structure and thermotropic properties of phosphatidylethanolamine and its N-methyl derivatives. *Biochemistry.* 23:2514–2519.

Nagel, N. E., G. Cevc, and S. Kirchner. 1992. The mechanism of the solute induced chain interdigitation in phosphatidycholine vesicles and characterization of the isothermal phase transitions by means of dynamic light scattering. *Biochim. Biophys. Acta.* 1111:263–269.

Nambi, P., E. S. Rowe, and T. J. McIntosh. 1988. Studies of the ethanol-induced interdigitated gel phase in phosphatidylcholines using the fluorophore 1,6-Diphenyl-1,3,5-hexatriene. *Biochemistry.* 27:9175–9182.

Ohki, K., K. Tamura, and I. Hatta. 1990. Ethanol induces interdigitated gel phase (I_{gi}) between lamellar gel phase ($L_{\beta'}$) and ripple phase ($P_{\beta'}$) in phosphatidylcholine membranes: a scanning density meter study. *Biochim. Biophys. Acta.* 1028:215–222.

Parsegian, A. V. 1983. Dimensions of the "intermediate" phase of dipalmitoylphosphatidylcholine. *Biophys. J.* 44:413–415.

Pascher, I., S. Sandell, and H. Hauser. 1981. Glycerol conformation and molecular packing of membrane lipids. *J. Mol. Biol.* 153:807–824.

Ranck, J. L., and J. F. Tocanne. 1982. Polymyxin B induces interdigitation in dipalmitoylphosphatidylglycerol lamellar phase with stiff hydrocarbon chains. *FEBS Lett.* 143:175–178.

Rand, R. P., and V. A. Parsegian. 1990. Hydration forces between phospholipid bilayers. *Biochim. Biophys. Acta.* 988:351–377.

Rowe, E. S. 1987. Induction of lateral phase separations in binary lipid mixtures by alcohol. *Biochemistry.* 26:46–51.

Rowe, E. S. 1983. Lipid chain length and temperature dependence of ethanol-phosphatidylcholine interactions. *Biochemistry.* 22:3299–3304.

Rowe, E. S. 1985. Thermodynamic reversibility of phase transitions. Specific effects of alcohols on phosphatidylcholines. *Biochim. Biophys. Acta.* 813:321–330.

Rowe, E. S., and T. A. Cutrera. 1987. Differential scanning calorimetric studies of ethanol interactions with destearoylphosphatidycholine: transition to the interdigitated phase. *Biochemistry.* 29:10398–10404.

Ruocco, M. J., and G. G. Shipley. 1982. Characterization of the subtransition of hydrated dipalmitoylphosphatidylcholine bilayers kinetik, hydration and structural study. *Biochim. Biophys. Acta.* 691:309–320.

Safinya, C. R., E. B. Sirota, D. Roux, and G. S. Smith. 1988. Universality in interacting membranes: the effect of cosurfactants on the interfacial rigidity. *Phys. Rev. Lett.* 62:1134–1137.

Simon, S. A., and T. J. McIntosh. 1984. Interdigitated hydrocarbon chain packing causes the biphasic transition behavior in lipid/alcohol suspensions. *Biochim. Biophys. Acta.* 773:169–172.

Slater, J. L., and C.-H. Huang. 1988. Interdigitated bilayer membranes. *Prog. Lipid Res.* 27:325–359.

Stamatoff, J., B. Feuer, H. J. Guggenheim, G. Tellez, and T. Yamane. 1982. Amplitude of rippling in the P_β phase of dipalmitoylphophatidylcholine bilayers. *Biophys. J.* 38:217–226.

Tardieu, A., and V. Luzzati. 1973. Structure and polymorphism of the hydrocarbon chains of lipids: a study of lecithin-water phases. *J. Mol. Biol.* 75:711–733.

Veiro, J. A., P. Nambi, and E. S. Rowe. 1988. Effect of alcohols on the phase transitions of dihexadecylphosphatidylcholine. *Biochim. Biophys. Acta.* 943:108–111.

Veiro, J. A., P. Nambi, L. L. Herold, and E. S. Rowe. 1987. Effect of *n*-alcohols and glycerol on the pretransition of dipalmitoylphosphatidylcholine. *Biochim. Biophys. Acta.* 900:230–238.

Weast, R. C., and M. J. Astle. 1978. Handbook of Chemistry and Physics. 26th Ed. CRC Press, Boca Raton, FL.

Wiener, M. C., R. M. Suter, and J. F. Nagle. 1989. Structure of the fully hydrated gel phase of dipalmitoylphosphatidylcholine. *Biophys. J.* 55:315–325.